CHEMISTRY
A EUROPEAN JOURNAL

ChemPubSoc
Europe

DOI: 10.1002/chem.201200096

# Correlating DFT-Calculated Energy Barriers to Experiments in Nonheme Octahedral $Fe^{IV}O$ Species

**Kyung-Bin Cho,[a] Eun Jeong Kim,[a] Mi Sook Seo,[a] Sason Shaik,*[b] and Wonwoo Nam*[a]**

**Abstract:** The experimentally measured bimolecular reaction rate constant, $k_2$, should in principle correlate with the theoretically calculated rate-limiting free energy barrier, $\Delta G^{\neq}$, through the Eyring equation, but it fails quite often to do so due to the inability of current computational methods to account in a precise manner for all the factors contributing to $\Delta G^{\neq}$. This is further aggravated by the exponential sensitivity of the Eyring equation to these factors. We have taken herein a pragmatic approach for C–H activation reactions of 1,4-cyclohexadiene with a variety of octahedral nonheme $Fe^{IV}O$ complexes. The approach consists of empirically determining two constants that would aid in predicting experimental $k_2$ values uniformly from theoretically calculated electronic energy ($\Delta E^{\neq}$) values. Shown in this study is the predictive power as well as insights into energy relationships in $Fe^{IV}O$ C–H activation reactions. We also find that the difference between $\Delta G^{\neq}$ and $\Delta E^{\neq}$ converges at slow reactions, in a manner suggestive of changes in the importance of the triplet spin state weight in the overall reaction.

**Keywords:** C–H activation · density functional calculations · kinetics · nonheme iron–oxo species · reaction rate

## Introduction

The relation between the free energy barrier ($\Delta G^{\neq}$) and the second-order reaction rate ($k_2$) in a chemical reaction is given by the Eyring equation:[1]

$$k_2 = \kappa \cdot k_B T/h \cdot \exp(-\Delta G^{\neq}/RT) \Leftrightarrow \ln k_2 = \ln(\kappa \cdot k_B T/h) - \Delta G^{\neq}/RT \quad (1)$$

Here $R$ is the gas constant, $T$ the temperature, $k_B$ the Boltzmann constant, and $\kappa$ a transmission coefficient that is usually set to 1. With quantum chemical tools such as density functional theory (DFT),[2] it is possible to calculate $\Delta G^{\neq}_{calcd}$ values routinely, and their quality can in principle be tested against known $k_2$ values though Equation (1). However, for complex systems, the calculated $\Delta G^{\neq}_{calcd}$ is quite often different from the measured $\Delta G^{\neq}_{exptl}$ due to many factors that are difficult to model in the calculations,[3] and one has quite often to rely on experiments or alternative theories.[4] For instance, loss of translational and rotational entropies upon association of the reactants is one of these factors that can influence the quality of $\Delta G^{\neq}_{calcd}$. Another factor that influences the trend is dispersion, which is usually calculated separately and requiring only the atomic coordinates.[5] Neglect of tunneling, counter ions[6] or interacting molecules further affects the accuracy.[6b,c] This is in addition to method-related errors due to the choice of functional, basis set, and solvation models. The difficulties and possible error sources in obtaining the experimental values should not be underestimated either. Thus, while calculations often give reliable trends, accurate specific numbers are still hard to come by. So the challenge is definitely daunting and awaiting a breakthrough in theoretical methods.

The introduction of transition-metal ions can cause additional problems, such as multi-spin state reactivities,[7] where the reaction mechanisms involve different spin states. This requires sometimes knowledge of spin inversion probability (SIP) to calculate the free-energy barriers correctly,[8] which would include high-level ab initio calculations to estimate the spin–orbit coupling (SOC).[9] Also, for highly charged species, the inclusion of reliable solvation models may become very important, to avoid self-interaction errors (SIE) in DFT.[6c,10] This is usually done with a dielectric medium included even during geometry optimizations. However, in doing so, other problems may arise. Adding thermal contributions then becomes in principle inaccurate since the

[a] Dr. K.-B. Cho, E. J. Kim, Dr. M. S. Seo, Prof. W. Nam
Department of Bioinspired Science
Ewha Womans University
120-750 Seoul (Korea)
Fax: (+82) 2-3277-4441
E-mail: wwnam@ewha.ac.kr

[b] Prof. S. Shaik
Institute of Chemistry and The Lise Meitner-Minerva
Center for Computational Quantum Chemistry
The Hebrew University of Jerusalem
91904 Jerusalem (Israel)
Fax: (+972) 2-6584680
E-mail: sason@yfaat.ch.huji.ac.il

Supporting information for this article is available on the WWW under http://dx.doi.org/10.1002/chem.201200096.

standard solvent models are parameterized to yield good solvation free energies and not any other property. This means that thermal effects are already included, to a certain extent, in the obtained electronic energies, hence possibly double counting the thermal contributions[11] (the same consideration applies to the dispersion correction as well). On the other hand, gas-phase frequency calculations on the so obtained structure may not be meaningful either since the structure may not be in a stationary point without the solvent. This leaves us in principle with no easily available options to calculate in a uniform manner the free energies and at the same time avoid SIE, for highly charge systems, unless one is prepared to enlarge the model system to include counter ions,[6b] which may be more time consuming and sometimes leading to 'reactions' between the transition-metal complex and the counter ions, which may or may not be realistic.

In principle, one could pursue the strategy of sorting out all these issues to obtain an accurate free-energy value. But even so, the ultimate accuracy is limited to the inherent accuracy of DFT.[10] Due to the exponential nature of Equation (1), every 1.4 kcal mol$^{-1}$ of error in the energy value translates into an error of one order of magnitude in reaction rates at room temperature. While highly sophisticated methods like CCSD(T) with complete basis set limit estimate can lead to more accurate barriers,[12] such methods are still inapplicable to transition-metal complexes in a routine manner. This leaves DFT as the default workhorse for doing the calculations. It has therefore been safer, at least for fast reactions, to compare two calculated barrier values to each other, rather than directly comparing the individual barriers to individual experimental values. This difference in barriers could be compared to corresponding relative experimental rate constants, taking advantage of cancellation of errors. However, our goal here is to compare the calculated energies directly to the $k_2$ values. As such, it is clearly desirable to seek a simplified and yet a predictive procedure that takes advantage of the advent of fast DFT calculations and usefully correlates theoretical results to experiments, while minimizing errors described above.

Computational investigations of the biologically relevant $Fe^{IV}O$ chemistry belong to the categories of calculations that contain all the computational difficulties described above. The importance of $Fe^{IV}O$ intermediates in biological systems is well documented; yet not complete owing to the vast range of occurrences and reactions it participates in. Most notably, it is either found or strongly implicated in important in vivo heme systems such as cytochrome P450,[13] horseradish peroxidise,[14] and nitric oxide synthase.[15] The $Fe^{IV}O$ species has also been shown to be of central importance in nonheme enzymes,[16] such as taurine:α-ketoglutarate dioxygenase,[17] prolyl-4-hydroxylase,[18] and halogenase CytC3.[19] Therefore, fundamental studies on such species are conducted in biomimetic settings as well, where simple models are replacing the complex enzymes.[20] Of particular interest for these synthetic nonheme $Fe^{IV}O$ complexes are their oxidizing powers. One way of measuring this is by their ability to hydroxylate a substrate. It has been shown, both theoretically[21] and experimentally[22] through C–H bond strength dependence and kinetic isotope effects, that the hydroxylation reaction occurs through a so called C–H activation step. The C–H activation step involves an H-atom transfer (HAT) from a substrate to the $Fe^{IV}O$ complex in a concerted proton coupled electron transfer (PCET) fashion,[6b,7b,23] followed by a rebound step. Since the C–H activation part is the rate-limiting step, it will determine the reactive power of the compound. Several nonheme compounds have been synthesized over the years to mimic the oxidation properties of $Fe^{IV}O$.[22,24] These compounds vary in oxidizing powers, the strongest found yet to be capable of C–H activating strong C–H bonds, such as in cyclohexane, at −40 °C.[24c] In many cases, however, simple comparisons between the compounds are difficult due to different experimental conditions, nascent from different substrates, solvents, labs, and/or arbitrary preferences. Theoretical investigations, while being informative about general reactivity trends, they still suffer from the above mentioned technical limitation to yield accurate rate constants.

We present herein a combined experimental and theoretical study of a series of 1,4-cyclohexadiene (CHD) C–H activation reactions by synthetic nonheme octahedral $Fe^{IV}O$ complexes with seven different ligands (Figure 1, **1**–**7** constituting our calibration set).[22,24c–e] These are verified $Fe^{IV}O$ compounds that were characterized with a multitude of experimental methods. The chosen complexes have all an active $Fe^{IV}O$ moiety with five nitrogen moieties bound to the iron, that is, $[N_5–Fe^{IV}O]^{2+}$, with some of the complexes having an acetonitrile solvent molecule that occupies the fifth coordination site (Figure 1). The five-coordination is determined in each of the seven cases by X-ray crystallography, EPR, and/or Mössbauer spectra.[22,24c–e] To compare the theoretical and experimental rates, we attempt to shortcut through the myriad of error sources, detailed above, by finding empirically determined parameters that would implicitly include all the corrective factors for the intended system. While this is not a strict theoretical approach to the problem, the aim is to create a practically useful approach, which this procedure will be seen to fulfill. Because of the semi-empirical nature, the resulting parameters can only be expected to work well for systems similar to the calibration set. Nevertheless, if it is indeed useful for the targeted system, then it may also serve as a springboard for further parameterizations on other systems. Finding empirical parameters requires the data points to be obtained from a uniform set of methods, which is what is done in this study. The seven compounds we use here are all treated equally, where the experimental $k_2$ values were determined using the same settings, and each computed electronic energy barriers ($\Delta E^{\ddagger}$) were determined using the same computational protocol. The number of different structures presented here includes for each of the seven compounds: the isolated $Fe^{IV}O$ species (without the substrate), reactants, transition states (TS), and products, in two multiplicities each (a total of 56 optimized geometries), constituting the calibration set. In

  

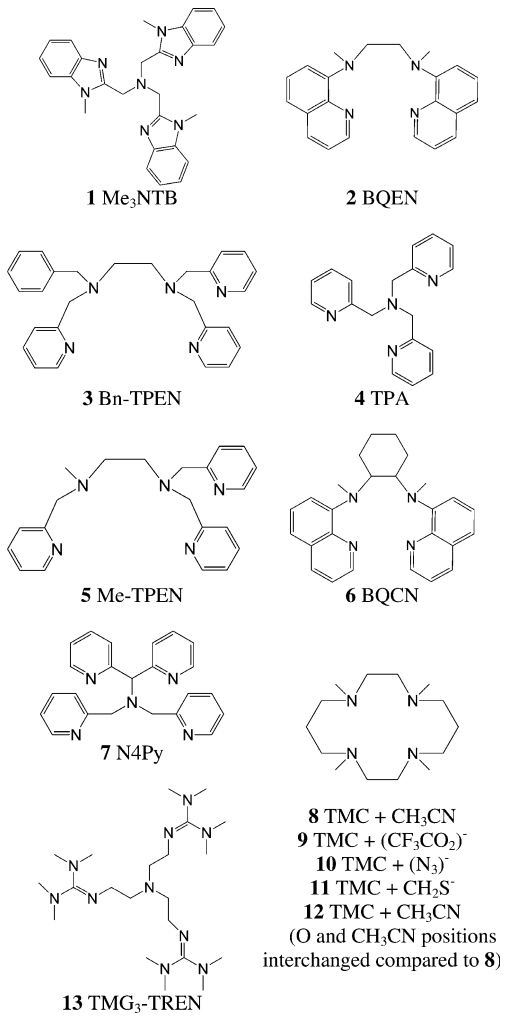


Figure 1. Different $[Fe^{IV}O(L)]^{2+}$ species used in this study, where L is the ligand system specified above. **1**–**7** constitutes the calibration set (Table 1) of ligands from which we approximated our empirical relationships, while **8**-**13** is the prediction set, in addition to some supplementary data for **1**, **2**, **3**, **4** and **7**, see Table 2. For structures **1**, **2**, **4**, and **6**, a solvent molecule ($CH_3CN$) was added at the fifth coordination site (see text). For explanations of ligand abbreviations, see the Supporting Information.

addition, some of the reactions in the prediction set have been calculated in the present study as well. Here, we address four main questions: 1) Based on the reactant structure of a specific $Fe^{IV}O$ species, can we say something about its reactivity compared to other $Fe^{IV}O$ structures with different ligands? 2) Can we predict its second order reaction rate constant $k_2$ based on this relationship? 3) Can we estimate $k_2$ values based on the calculated energy barriers better than the Eyring equation? 4) What physical insights can we obtain from these procedures?

## Results and Discussion

**Orbitals, geometries, and spin density distributions**: The molecular orbitals involved in C–H activation reactions by

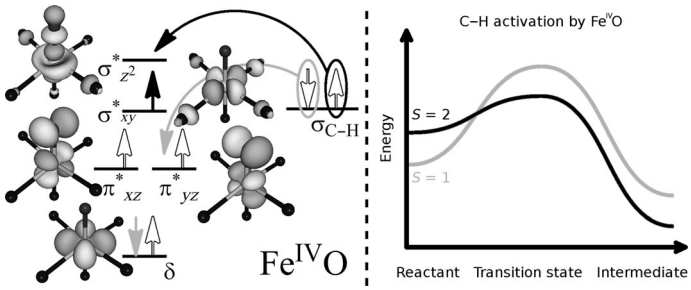


Figure 2. Valence electron orbital occupations in a typical nonheme $Fe^{IV}O$ system (left). Grey+white indicate low-spin ($S=1$) population, while black+white indicate high-spin ($S=2$) population. During C–H activation, a β-electron is shifted to one of the π* orbitals in the low-spin state, while an α-electron is shifted to the $\sigma^*_{z^2}$ orbital in the high-spin case. A typical generic reaction energy profile for C–H activation is shown (right), where the reactant state is in its low-spin state (gray), while the reaction itself occurs through the high-spin state (black) due to its lower energy barrier.

$Fe^{IV}O$ species have been extensively reviewed before.[8,6b] Generally, the low-spin state ($S=1$) is energetically favored at the reactant stage, with a valence orbital occupation of ($\delta^2$, $\pi^*_{xz}{}^1$, $\pi^*_{yz}{}^1$), see Figure 2. However, at the TS region (Figure 3), the high-spin configuration ($S=2$) is preferred due to larger exchange interaction energy caused when an α-electron is shifted from the substrate to the FeO moiety,[6b] resulting in an FeOH intermediate with a configuration of ($\delta^2$, $\pi^*_{xz}{}^1$, $\pi^*_{yz}{}^1$,$\sigma^*_{xy}{}^1$,$\sigma^*_{z^2}{}^1$). Hence, a spin-state shift occurs during the reaction, and by estimating the size of the SOC constant in a reaction with a bare $FeO^+$ system,[9c,d] it was concluded that this shift was more likely to occur before the TS. For HAT reactions of $Fe^{IV}O$ systems, it was argued that there are two possible scenarios;[21,25] one involves spin pre-equilibrium near the reactants, the other involves spin flip en-route to the TS, with SIP which can be significantly smaller than 1. A recent study of HAT reactions by $Mn^{V}O$ revealed a case in which the minimum energy crossing point (MECP[26]) was close to the TS.[25] The former scenario was recently implied in $Co^{II}H_2bim$ systems as well.[27] Both scenarios are indeed possible.

Some general features can be attributed to all the calculated $Fe^{IV}O$ species. For instance, the Fe–O distances are all found to be 1.65 or 1.66 Å with or without the weakly bonded substrate nearby and regardless of spin quantum number. Also, the combined $Fe^{IV}O$ spin density distribution is 2.09–2.21 for low-spin and 3.68–3.82 for high-spin. These variations, however, do not seem to affect reactivity patterns. One might have also expected that the high-spin $Fe-N_{axial}$ bond length may offer some clue about reactivity patterns, since this parameter affects the level of the $\sigma^*_{z^2}$ orbital that is getting filled during the reaction. This bond length was however found to vary unsystematically between 2.07–2.17 Å. Hence, we conclude that there are no obvious features of the isolated low-spin $Fe^{IV}O$ compound that would give a useful clue about its reactivity. Nevertheless, as shown below, the calculated triplet–quintet energy gap correlates well with the reactivity ordering in the series.

  

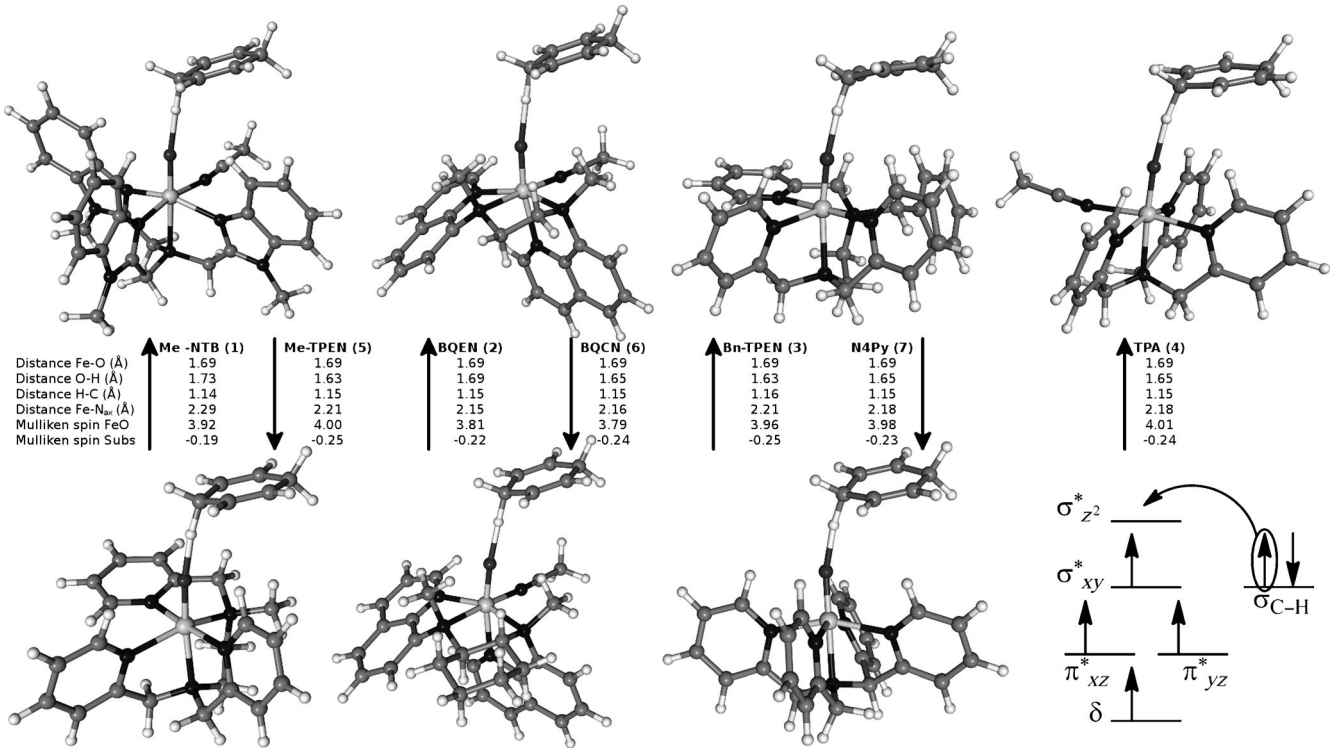


Figure 3. Selected geometries and Mulliken spin density distribution for $S=2$ transition states (see also the Supporting Information). The electron shift diagram for the quintet state is shown.

**Empirically modified Eyring equation**: Our initial approach is to first examine the quality of the calculated barrier values vis-à-vis experimentally obtained $k_2$ values. As already mentioned, the exponential nature of the Eyring equation can cause the discrepancy to go off scale. This is seen to occur in Table 1 where Equation (1) is used with calculated free energy barriers ($\Delta G^{\neq}_{calcd}$) for the calibration set. The predicted $k_2$ deviates up to nine orders of magnitude off the experimental values. This expected failure of $\Delta G^{\neq}_{calcd}$ values to match the experimental rate constants underscores the need for a useful correlation. In a move to simplify the discussion, we will henceforth use only the electronic energy $\Delta E^{\neq}$ rather than $\Delta G^{\neq}_{calcd}$, with $\Delta E^{\neq}$ consisting of only the electronic energy at the B3LYP/LACV3P**+ //B3LYP/LACVP level of theory[28] in acetonitrile (see the Experimental Section for details). Such a simplification is justified here based on the fact that the calculated $\Delta G^{\neq}_{calcd}$ does not result in an improved quality of $k_2$, notwithstanding the question of validity of such calculations on solvent-included systems.[11] Hence, the attractiveness of the scheme described below will rest on the ease of calculating electronic energies $\Delta E^{\neq}$.

Our first effort to improve the quality of the experimental versus theoretical correlation begins with a modification to the logarithmic form of the Eyring equation. Noting that it is a linear equation with $\Delta E^{\neq}$ as an independent variable, we set $\kappa=1$ and introduce two empirical correction constants A and $\varepsilon$ which will change the intercept (pre-exponential factor) and the slope (the calculated energy), respectively:

$$\ln k_2 = [\ln(k_B T/h) - A] - (1-\varepsilon)/RT \cdot \Delta E^{\neq} \quad (2)$$

Hence, in the ideal case of perfect theory–experiment match, $\Delta E^{\neq}$ would be exactly $\Delta G^{\neq}_{exptl}$, leading to $A=0$ and $\varepsilon=0$. This will however not be

Table 1. Predictions on the calibration set[a] with Equations (1) and (2) using theoretical ($\Delta^5 E^{\neq}/\Delta G^{\neq}_{calcd}$) values.

| | $\Delta^5 E^{\neq}$ [kcal mol$^{-1}$][b] | $\Delta G^{\neq}_{calcd}$ [kcal mol$^{-1}$][b] | $\Delta G^{\neq}_{exptl}$ [kcal mol$^{-1}$][c] | Exptl $k_2$ [$M^{-1}s^{-1}$][b] | [Eq. (1)] [$M^{-1}s^{-1}$][d] | **[Eq. (2)] [$M^{-1}s^{-1}$]**[e] |
|---|---|---|---|---|---|---|
| **1**[f] | 5.27 | 0.43 | 10.4 | $9.4(\pm0.3)\times10^2$ | $1.9\times10^{12}$ | **77** |
| **2** | 7.00 | 2.13 | 12.5 | $1.0(\pm0.1)\times10^1$ | $4.9\times10^{10}$ | **19** |
| **3**[f] | 6.97 | 2.36 | 12.7 | $5.7(\pm0.2)$ | $3.0\times10^{10}$ | **20** |
| **4** | 9.96 | 3.22 | 12.8 | $5.3(\pm0.2)$ | $4.6\times10^9$ | **1.8** |
| **5** | 7.26 | 2.95 | 12.8 | $5.0(\pm0.2)$ | $8.3\times10^9$ | **16** |
| **6** | 8.75 | 3.79 | 13.3 | $1.5(\pm0.1)$ | $1.4\times10^9$ | **4.8** |
| **7**[f] | 12.34 | 8.67 | 13.8 | $5.3(\pm0.2)\times10^{-1}$ | $3.6\times10^4$ | **0.28** |

[a] Uniform set of theory and methods at −40 °C. [b] See Experimental Section for details. [c] Obtained via Equation (1) from experimental $k_2$. [d] Predicted $k_2$ using $\Delta G^{\neq}_{calcd}$ and Equation (1). [e] Predicted $k_2$ using calculated $\Delta^5 E^{\neq}$ and Equation (2). [f] Experimental and some of the theoretical data published elsewhere.[24c]

  

the case as $\Delta E^{\neq}$ in general is a rather crude approximation for $\Delta G^{\neq}_{exptl}$. Therefore, we expect the A and $\varepsilon$ terms to play a vital role in this correlation and hopefully also enhance our understanding of the currently studied system. Rearranging Equation (2), we can express it in the equivalent form:

$$\ln k_2 = \ln(k_B T/h) - [((1-\varepsilon)\Delta E^{\neq} + A \cdot RT)/RT] \quad (3)$$

Comparing Equation (3) to Equation (1), we can see that the second term leads to:

$$\Delta G^{\neq}_{exptl} = (1-\varepsilon)\Delta E^{\neq} + A \cdot RT = \Delta E^{\neq} - \varepsilon \Delta E^{\neq} + A \cdot RT \quad (4)$$

where $\Delta G^{\neq}_{exptl}$ is available either from an Eyring plot ($\ln k_2$ vs. $1/T$) or from Equation (1), using the measured $k_2$ at a certain temperature (in the current study, both methods yield the same $\Delta G^{\neq}_{exptl}$ values within 0.1 kcal mol$^{-1}$, see Tables S61 and S62 in the Supporting Information). Equation (4) highlights a possible linear relationship between the free and electronic energies (Figure 4), which is known in physical organic chemistry (the isokinetic relationship), and implies that the correction constants may have some physical significance.

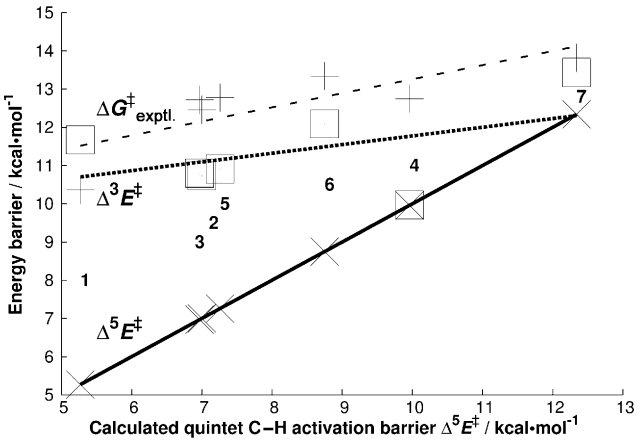


Figure 4. Plots showing correlations in the C–H bond activation of CHD by $[FeO^{IV}(L)]^{2+}$. The calculated quintet state barrier ($\Delta^5E^{\neq}$) is correlated versus itself (full, ×), the triplet barrier $\Delta^3E^{\neq}$ (dotted, □) and the experimental free energy $\Delta G^{\neq}_{exptl}$ (dashed, +). $\Delta G^{\neq}_{exptl}$ converted from $k_2$ via Equation (1) is correlated to $\Delta^5E^{\neq}$, giving $\Delta G^{\neq}_{exptl} = 0.3687 \cdot \Delta^5E^{\neq} + 9.57$ with $R^2 = 0.63$. $\Delta^3E^{\neq}$ is also fitted to a line $\Delta^3E^{\neq} = 0.227 \cdot \Delta^5E^{\neq} + 9.50$. Although the latter fitting is poor ($R^2 = 0.22$), the standard deviation to the average value is small (1.1 kcal mol$^{-1}$) and the trend is clear.

**Correlating theory and experiment**: Figure 4 shows linear regression correlated line between the calculated quintet state barrier ($\Delta^5E^{\neq}$) versus itself, the triplet barrier ($\Delta^3E^{\neq}$) and $\Delta G^{\neq}_{exptl}$. Comparing the two spin states, one can see that the quintet barrier is consistently lower over the calibration set, as expected. Hence, if assuming a spin inversion probability of 1, the barrier of the reactions can indeed be considered to be mediated solely by the quintet state and therefore, $\Delta E^{\neq}$ is equal to $\Delta^5E^{\neq}$ in the current study. As already apparent from the figure, and as we shall discuss later, $\Delta^5E^{\neq}$ and $\Delta G^{\neq}_{exptl}$ (and also $\Delta^3E^{\neq}$) are seen to converge at higher $\Delta^5E^{\neq}$, which may be a consequence of spin inversion probability deviating from unity.

The correlations of $\Delta^5E^{\neq}$ versus $\Delta G^{\neq}_{exptl}$ and $\Delta^3E^{\neq}$ yield the equations:

$$\Delta G^{\neq}_{exptl} = 0.3687 \cdot \Delta^5E^{\neq} + 9.57 \quad (5a)$$

$$\Delta^3E^{\neq} = 0.2270 \cdot \Delta^5E^{\neq} + 9.50 \quad (5b)$$

The correlation coefficient of $R^2 = 0.63$ for Equation (5a) shows that while a trend exists, the correlation is not too good. Still, for our purposes this may suffice. Setting Equation (5a) equal to Equation (4) provides the values of A and $\varepsilon$ as 20.67 and 0.6313, respectively. Once these correction 'constants' are found, Equation (2) enables us to predict experimental $k_2$ values, given the calculated $\Delta^5E^{\neq}$. As expected, the predicted values with Equation (2) on the calibration set are reasonably acceptable (see last column in Table 1). Even with **1**, which exhibits an extremely fast reaction rate, the prediction is accurate to one order of magnitude. Furthermore, the usefulness of Equation (2) is underscored by the prediction set (Table 2) of 14 reactions,[7b,8,22,24c,e,29] which to the best of our knowledge contain all nonheme synthetic $Fe^{IV}O$ complexes for which both experimental $k_2$ and theoretical $\Delta^5E^{\neq}$ is available. One has to remember that in this set, the methods used to obtain the experimental and theoretical values are no longer uniform and may differ signifi-

Table 2. Predictions on the prediction set[a] with Equations (1) and (2) using theoretical ($\Delta^5E^{\neq}/\Delta G^{\neq}_{calcd}$) values.

| | $\Delta^5E^{\neq}$ [kcal mol$^{-1}$] | $\Delta G^{\neq}_{calcd}$ [kcal mol$^{-1}$] | $T$ [°C][b] | Exptl $k_2$ [M$^{-1}$s$^{-1}$] | [Eq. (1)] [M$^{-1}$s$^{-1}$][c] | **[Eq. (2)] [M$^{-1}$s$^{-1}$][d]** |
|---|---|---|---|---|---|---|
| **1**[e,f] | 12.6 | 3.6 | −40 | 0.25 | $1.9\times10^{9}$ | **0.22** |
| **1**[g–i] | 9.8 | 4.4 | −40 | 1.5 | $4.0\times10^{8}$ | **2.2** |
| **2**[g,h,j] | 12.4 | 8.1 | 0 | $2.6\times10^{-2}$ | $1.9\times10^{6}$ | **1.3** |
| **3**[e,h,k] | 14.2 | 8.1 | 25 | $3.9\times10^{-4}$ | $7.0\times10^{6}$ | **0.93** |
| **4**[f,g] | 14.5 | 9.6 | −40 | $3.0\times10^{-3}$ | $4.6\times10^{2}$ | $\mathbf{4.7\times10^{-2}}$ |
| **7**[e,h,k] | 19.1 | 13.2 | 25 | $5.5\times10^{-5}$ | $1.4\times10^{3}$ | $\mathbf{4.6\times10^{-2}}$ |
| **7**[l] | 10.8 | 6.5 | −30 | 1.3 | $7.2\times10^{6}$ | **1.4** |
| **8**[l] | 12.0 | 7.1 | −30 | $1.8\times10^{-2}$ | $2.1\times10^{6}$ | **0.56** |
| **8**[m] | 12.5 | 17.1 | 0 | 0.12 | 0.12 | **1.2** |
| **9**[m] | 10.5 | 17.4 | 0 | 1.3 | $6.7\times10^{-2}$ | **4.8** |
| **10**[m] | 10.7 | 20.1 | 0 | 1.4 | $4.6\times10^{-4}$ | **4.2** |
| **11**[m,n] | 13.0 | 21.6 | 0 | 6.1 | $2.9\times10^{-5}$ | **0.87** |
| **12**[n,o] | 7.5 | n. a. | 0 | 22 | n. a. | **37** |
| **13**[l] | 14.9 | 15.6 | −30 | 1.2 | $4.7\times10^{-2}$ | $\mathbf{6.1\times10^{-2}}$ |

[a] Mostly literature data. [b] Temperature used in experiments and prediction. [c] Predicted $k_2$ using $\Delta G^{\neq}_{calcd}$ and Equation (1). [d] Predicted $k_2$ using calculated $\Delta^5E^{\neq}$ and Equation (2). [e] Using cyclohexane as substrate. [f] Data from this study. [g] Using ethylbenzene as substrate. [h] Theoretical data from this study. [i] Experimental data from ref. [24c]. [j] Experimental data from ref. [24e]. [k] Experimental data from ref. [22]. [l] Experimental data from ref. [29a] and theoretical data from ref. [7b]. [m] Data from ref. [8]. [n] Using 9,10-dihydroanthracene as substrate, assuming that the similar C–H bond strength will give the same barrier height as CHD. [o] Experimental data from ref. [29b] and theoretical data from ref. [29c].

cantly from what the correction constants were calibrated for. Nevertheless, the same A and $\varepsilon$ constants in Equation (2) seem to work well for CHD in this set. Specifically, small changes in temperature (**7** in Table 1 vs. seventh row in Table 2) and/or theoretical solvent modeling (the two **8**) seem to keep the correlation at acceptable levels. Even in the cases where the axial ligand is not a nitrogen (**9** and **11**), or when it is loosely bound (ca. 2.2 Å in **12**) seem to give reasonable predictions.

Table 2 contains also entries with substrates other than CHD. The predictions seem to hold when the substrate is 9,10-dihydroanthracene (**11** and **12**), which has a similar C–H bond strength as CHD. Using ethylbenzene, it can be seen that **1** and **4** (second and fifth row) also fit fairly well to the model. However, the prediction for **2** (where the substrate is also ethylbenzene) is two orders of magnitude off. Using cyclohexane as substrate, **1** (first row) gives a reasonable prediction while **3** and **7** (fourth and sixth rows) give the worst predictions in the set.

Hence, the conclusion of this procedure is that for CHD or other substrates with similar C–H bond strengths, usage of Equation (2) reduces the error to within one order of magnitude from the experimental values of $k_2$. This is equivalent to about 1.4 kcal mol$^{-1}$ error in the barrier energies, which is favorably comparable to the expected standard error in calculations of $\Delta G^{\neq}_{calcd}$. The results also indicate a progressive dependence of the accuracy versus C–H bond strength difference; from a good agreement for weak C–H bonds that it was parameterized for, to an average agreement for a moderately stronger C–H bond strength (ethylbenzene, two out of three predicted values acceptable) to a less than good agreement for strong C–H bond strengths (cyclohexane, one out of three predictions acceptable). It should be noted here that the experimental $k_2$ values for all the agreeing cases above were determined at identical experimental conditions as in the calibration set, while all the non-compatible cases uses different experimental settings. Still, deviations on systems for which it was not parametrized for (i.e., stronger C–H bonds) are not unreasonable, and may require future separate calibrations, or inclusion of a more mixed substrate set in the calibration set to improve the agreement. Finally, an additional case of disagreement is **13**,[29a,7b] which is a trigonal bipyramidal system that is fundamentally different from the octahedral system for which the calibration was done. However, even in this case, the prediction is not worse than what would be using no correction constants.

**O–H bond strength dependence**: It is of interest to explore how far we can simplify our predictive procedure, given that we have a set of uniform experimental data that we can test on. The Bell–Evans–Polanyi principle[30] suggests that reaction energy barriers may be proportional to the bond dissociation energy of the forming O–H bond ($BDE_{OH}$). We can therefore attempt to explore such a relationship, and start by establishing whether the calculated data exhibit such a correlation. As Figure 5 shows, there is an excellent correlation between the calculated energy barrier $\Delta^5E^{\neq}$ and $BDE_{OH}$ according to Equation (6a):

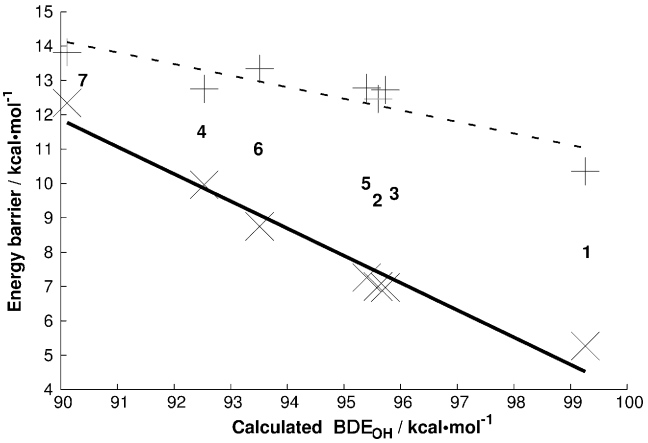


Figure 5. Correlating calculated O–H bond strengths to energy barriers. Electronic $BDE_{O-H}$ is correlated to the calculated (full, ×) and experimental (dashed, +) barrier heights, resulting in Equations (6a) and (6b) ($R^2=0.96$ and $R^2=0.80$, respectively).

$$\Delta^5E^{\neq} = -0.7923 \cdot BDE_{OH} + 83.17 \quad (6a)$$

Further, making a direct fit between calculated electronic $BDE_{OH}$ and experimental $k_2$, here translated to $\Delta G^{\neq}_{exptl}$ via Equation (1), Equation (6b) can be derived:

$$\Delta G^{\neq}_{exptl} = -0.3365 \cdot BDE_{OH} + 44.44 \quad (6b)$$

As a comparison, applying the $\Delta^5E^{\neq}$ expression of Equation (6a) in Equation (4) above results in $\Delta G^{\neq}_{exptl} = -0.2921 \cdot BDE_{OH} + 40.23$ at −40 °C (where $A \cdot RT = 9.57$), which is close to Equation (6b).

As shown by Equations (6a) and (6b), there seems to be different slopes and intercepts depending on the usage of $\Delta G^{\neq}_{exptl}$ or $\Delta^5E^{\neq}$. Here, the slope of −0.3 in Equation (6b) is markedly different from that of Equation (6a), which correlates electronic energies only, with a slope of −0.8. The difference in the slope term is thus about $0.5 \cdot BDE_{OH}$. Hence, while obtaining a linear correlation seems to be easy, a careful consideration of the kind of energies used in both sides of a correlating equation may be warranted, with no a priori assumption of the expected slope value as this can vary considerably depending on the kinds of energies used. The same consideration applies to the intercept as well.

**Reactant and TS spin state gap**: It is further instructive to look at yet another correlation. It has been repeatedly shown that for nonheme $Fe^{IV}O$ species like the ones in the present study, the reactant ground state is a low-spin triplet ($S=1$) state, while the lowest energy TS is the high-spin quintet ($S=2$) state.[7c,8] Hence, a spin state transition from $S=1$ to $S=2$ has to occur during the reaction. Since the barrier on the quintet state surface (relative to the quintet reactant) is small, the spin state gap at the reactant state

  

($\Delta E_{QT}{}^{R}$) will constitute a large part of the energy barrier (assuming SIP of unity or spin pre-equilibrium[8,21]). As such, we might expect a correlation between $\Delta E_{QT}{}^{R}$ and the barrier height. Figure 6 shows that the theoretically calculated barrier $\Delta^5E^{\neq}$ is excellently correlated to $\Delta E_{QT}{}^{R}$ ($R^2=0.96$), while the correlation to the experimental $\Delta G^{\neq}$ is not good ($R^2=0.45$):

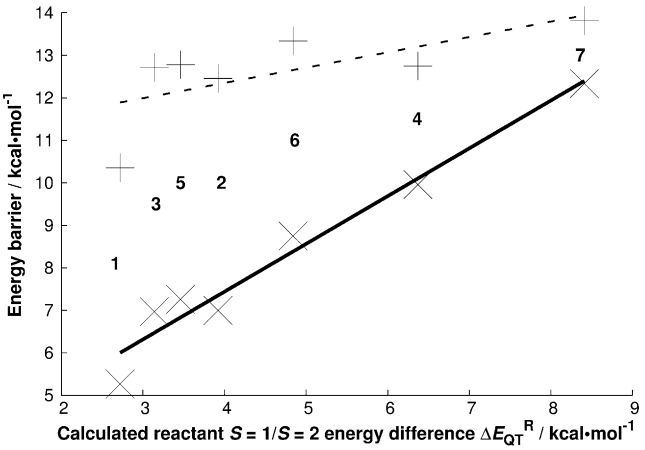


Figure 6. Correlating calculated $\Delta E_{QT}{}^{R}$ to energy barriers. The reactant spin state differences ($\Delta E_{QT}{}^{R}={}^5E-{}^3E$) were correlated against the calculated (full,×) and experimental (dashed,+) barriers resulting in Equations (7a) and (7b) ($R^2=0.96$ and $R^2=0.45$, respectively).

$$\Delta^5E^{\neq} = 1.125 \cdot \Delta E_{QT}{}^{R} + 2.94 \quad (7a)$$

$$\Delta G^{\neq}{}_{exptl} = 0.3600 \cdot \Delta E_{QT}{}^{R} + 10.91 \quad (7b)$$

Equation (7b) is close to $\Delta G^{\neq}{}_{exptl} = 0.4147 \cdot \Delta E_{QT}{}^{R} + 10.65$, which we obtain if we apply Equation (7a) in Equation (4).

Extending this idea to transition states, we can look at the spin state energy differences at the TS geometry ($\Delta E_{QT}{}^{TS}$). It is clear from Figure 6 that the larger $\Delta E_{QT}{}^{R}$, the larger are the barriers $\Delta^5E^{\neq}$ and $\Delta G^{\neq}{}_{exptl}$. At the same time, Figure 4 shows that the larger the barriers ($\Delta^5E^{\neq}$ or $\Delta G^{\neq}{}_{exptl}$), the smaller the spin-state gap becomes at the TS ($\Delta E_{QT}{}^{TS}$). Therefore, larger $\Delta E_{QT}{}^{R}$ implies smaller $\Delta E_{QT}{}^{TS}$. This is because increasing $\Delta E_{QT}{}^{R}$ is equivalent to increasing the *d*-orbital energy gaps, and the favorable exchange enhanced reactivity[31] on the high-spin state is then gradually counterbalanced and the both TSs converge.

**Potential insight**: While predicting experimental $k_2$ values is in itself important, we would like to explore the additional insight these correction constants may enfold. This may be achieved by examining Equation (4) closely. The free energy is expressed here as a linear function of the electronic energy $\Delta^5E^{\neq}$ with the slope $(1-\varepsilon)$ and a constant part $A{\cdot}RT$. Hence, Equation (4) divides the free energy into two parts; one part that is proportional to the numerical value of the electronic energy ($\Delta^5E^{\neq}$), and another part that is constant at the given temperature ($A{\cdot}RT$). Both parts should be a mix of different effects, but if we reason carefully, we may be able to pinpoint major contributions to each term. Superficially, the intercept term $A{\cdot}RT$ in Equation (4) appears as a temperature-dependent term, but strictly speaking, since A is determined at a specific temperature, the $A{\cdot}RT$ term is a constant. For **1–7**, Equation (4) with $A=20.67$ leads to an $A{\cdot}RT$ term of 9.57 kcal mol$^{-1}$ at −40 °C. The average $-T\Delta S^{\neq}$ based on our experiments is $6.5\pm3.2$ kcal mol$^{-1}$ (Table 3).

Table 3. Experimentally measured activation parameters at −40 °C.

| Ligand | $\Delta H^{\neq}$ [kcal mol$^{-1}$] | $\Delta S^{\neq}$ [cal K$^{-1}$ mol$^{-1}$] | $-T\Delta S^{\neq}{}_{233K}$ [kcal mol$^{-1}$] |
|---|---|---|---|
| **1** | 10.2 | −1.0 | 0.2 |
| **2** | 5.8 | −28.6 | 6.7 |
| **3** | 4.3 | −36.1 | 8.4 |
| **4** | 4.4 | −35.7 | 8.3 |
| **5** | 4.6 | −34.8 | 8.1 |
| **6** | 4.3 | −38.9 | 9.1 |
| **7** | 9.4 | −19.1 | 4.5 |
| **average** | **6.1** | **−27.7** | **6.5** |

Hence, the majority of the $A{\cdot}RT$ term seems to reflect entropy contributions. However, this number would also contain quasi-constant terms, such as zero-point vibrational energy effects $\Delta Z_0$, which is not temperature dependent and for our calibration set should not vary too much. Indeed, the calculated $\Delta Z_0$ is fairly constant across the calibration set (3.30–3.89 kcal mol$^{-1}$) without any systematic variation.

The physical meaning of the constant $\varepsilon$ is on the other hand not straightforward. The $-\varepsilon\Delta^5E^{\neq}$ term implies a downsizing effect that is proportional to the electronic energy barrier of the system. Tentatively the dispersion effect could be a candidate for it. However, for our systems, where we have $\Delta^5E^{\neq}$ in the range of 5–12 kcal mol$^{-1}$, $\varepsilon=0.63$ means that the $\varepsilon\Delta^5E^{\neq}$ term is in the 3–8 kcal mol$^{-1}$ range, which is well above our calculated dispersion effects (0–2 kcal mol$^{-1}$, see Figure S1 and S2 in the Supporting Information). Hence, there must be some additional effects. Having already accounted for $\Delta Z_0$, entropy and dispersion effects, expected major contributions unaccounted for would be the thermally dependent enthalpy and SIP. The former factor is usually negligible and is indeed only in the 0.1–0.5 kcal mol$^{-1}$ range for our calibration set. Could then the factor $(1-\varepsilon)$ be related to SIP? In the following discussion we show that this effect is plausible.

As we discussed above by reference to Figure 4, the $\Delta G^{\neq}{}_{exptl}$ and $\Delta^5E^{\neq}$ values converge, as the difference of $\Delta^3E^{\neq}$ and $\Delta^5E^{\neq}$ gets smaller. This can be most simply expressed as follows:

$$\Delta G^{\neq}{}_{exptl} - \Delta^5E^{\neq} = x(\Delta^3E^{\neq} - \Delta^5E^{\neq}) + c \quad (8a)$$

where $x$ and $c$ are constants. Equation (8a) rearranges into Equation (8b):

$$\Delta G^{\ddagger}_{\text{exptl}} = [(1-x)\Delta^5 E^{\ddagger} + x\Delta^3 E^{\ddagger}] + c \quad (8b)$$

The part in brackets is an expression for the electronic energy as a blend of the two spin state barriers, with the constant $c$ making up for the average deficiency arising in use of $\Delta E^{\ddagger}$ instead of $\Delta G^{\ddagger}$. Hence, $x$ is approximately the fraction of reactions occurring in the triplet state (as results of SIP, but other factors contribute as well). The $\varepsilon$ factor in Equation (4) can be easily deduced to be related to $x$ (see the Supporting Information).

It is imperative to point out that the above discussion is ultimately based on the assumption that the sampled points are on a line, that is, the linear approximation. It is shown to be valid in Figure 4 over a broad range of $\Delta^5 E^{\ddagger}$ for CHD (5 to 13 kcal mol$^{-1}$), but it remains nevertheless an approximation, and therefore it must be considered tentative. However, accepting this limitation, we can make progress in not only predicting $k_2$ values, but also in showing that spin state mixing may perhaps have a larger role than hitherto considered. This is because $x$ can be calculated from the correlation to be around 0.7 (see the Supporting Information). Therefore, Equation (8) surprisingly suggests a blended reactivity with a dominant triplet state contribution (on average, over the entire calibration set). Another possible interpretation of Equation (8b) is that it is not a true physical blending of the two spin state reactions but rather an effective correction of the $\Delta^5 E^{\ddagger}$ barrier due to over-stabilization of the high spin TS by B3LYP, although this latter interpretation needs further verifications, and is not at all certain.[6d] In any event, it remains true that the electronic energy $\Delta^5 E^{\ddagger}$ is a better approximation to $\Delta G^{\ddagger}_{\text{exptl}}$ at higher $\Delta^5 E^{\ddagger}$ values.

## Conclusion

Access to a common set of data obtained by identical methods enables us to investigate trends that are statistically relevant. We have generated seven sets of data, both experimentally and theoretically, using identical methods. This set contains synthetic nonheme octahedral $Fe^{IV}O$ species with an electronic energy reaction barrier for C–H activation of CHD in the calculated range of 5–13 kcal mol$^{-1}$. We investigated a relationship between $\Delta E^{\ddagger}$ and $\Delta G^{\ddagger}_{\text{exptl}}$ and found correlations that lead to improved predictions of these C–H activation barriers. We presented here three routes to predict the experimental reactivity based on correlations: 1) Calculate the relatively easily obtained electronic energy barrier $\Delta^5 E^{\ddagger}$ by DFT and then use Equation (4) to obtain $\Delta G^{\ddagger}$ and/or $k_2$; 2) use the Bell–Evans–Polanyi principle, calculate the O–H bond strengths, and use Equation (6b) if considering reactions conducted at −40 °C, or 3) with less accuracy and only for CHD as substrate, one can calculate the reactant $S=1/S=2$ spin state gap and then use Equation (7b). We also show that within the linear equation approximation, the spin state weight is more important for smaller calculated barriers (i.e. fast reactions). This is because the TS gap between the two spin states diminishes as the calculated barrier increases, effectively rendering the spin state identity less important. Also, we show that for slow occurring reactions the electronic energy is a useful approximation to the free energy.

## Experimental Section

**Theoretical methods**: Density functional theory (DFT)[2] was applied at the B3LYP/LACV3P**+//B3LYP/LACVP level[28] using Gaussian 09.[32] In previous trials, we have found that using gas-phase optimizations for highly charged species such as the current system (2+) caused a hydride transfer (i.e., one proton and two electrons) rather than a net hydrogen atom transfer from the substrate to the $Fe^{IV}O$ due to self-interaction errors. Performing the optimizations in solvent avoids these artificial results for the H-abstraction step;[6b] hence the solvent (acetonitrile) effects were included using CPCM model with UFF cavity, per G09 default.

Throughout this study, we use the electronic energy barriers ($\Delta E^{\ddagger}$) without any correction factors (except for solvent modeling, which is included by default on all calculations) due to its simplicity, both in calculation and analysis. For instance, the triplet reactant complex (RC) state (where the reagent and the substrate are weakly interacting) is always lower than its quintet counterpart at this level (see Tables S1–S20 in the Supporting Information), and the quintet TS is always lower than the triplet, hence the barrier height is always given by:

$$\Delta E^{\ddagger} = {}^5E_{\text{TS}} - {}^3E_{\text{RC}}$$

To do the comparison in Table 1, we calculate also the free energy barriers, $\Delta G^{\ddagger}_{\text{calcd}}$ (see discussion of Table 1). In doing these calculations, one has to decide what terms to include in $\Delta G^{\ddagger}_{\text{calcd}}$. Conventional calculations usually include $\Delta E^{\ddagger}$, zero-point vibrational energy ($\Delta Z_0{}^{\ddagger}$), enthalpy ($\Delta E_{\text{thermal}}{}^{\ddagger}$) and entropy ($-T\Delta S^{\ddagger}$) corrections. We have here also added dispersion effects, using the DFT-D3 program.[5] Adding all these effects, one could quite frequently end up with the result that complexation is an endothermic process (which also needs to be corrected by a factor $RT\cdot\ln 24.5$ due to change of standard state). One should keep in mind however, that the usage of the calculated free energies in this study is very limited due to all the difficulties detailed in the introduction, and any slight variation to the above described free energy calculation procedure would not likely change our conclusions.

**Experiments**: Commercially available chemicals were used without further purification unless otherwise indicated. Solvents were dried according to published procedures and distilled under Ar prior to use.[33] Peracetic acid ($CH_3CO_3H$, 32 wt % solution containing <6 % $H_2O_2$) was obtained from Aldrich Chemical Co. *m*-chloroperbenzoic acid (*m*-CPBA) was purified by washing with phosphate buffer (pH 7.4), followed by water and then dried under reduced pressure.[34]

  

Iodosylbenzene (PhIO) was prepared by literature methods.[35] Ligands and iron(II) complexes, $[Fe^{II}(Me_3NTB)(CH_3CN)](CF_3SO_3)_2$, $[Fe^{II}(BQEN)(CH_3CN)_2](CF_3SO_3)_2$, $[Fe^{II}(Bn\text{-}TPEN)](CF_3SO_3)_2$, $[Fe^{II}(TPA)(CH_3CN)_2](ClO_4)_2$, $[Fe^{II}(Me\text{-}TPEN)](CF_3SO_3)_2$, $[Fe^{II}(BQCN)(CH_3CN)_2](CF_3SO_3)_2$, and $[Fe^{II}(N4Py)](CF_3SO_3)_2$ were prepared by literature methods.[22,24c–e,36]

UV/Vis spectra were recorded on a Hewlett Packard 8453 diode array spectrophotometer equipped with a UNISOKU Scientific Instruments Cryostat USP-203 A for low-temperature experiments or on a Hi-Tech Scientific (U.K.) SF-61 DX2 cryogenic stopped-flow spectrometer equipped with a Xe arc lamp and a KinetaScan diode array rapid scanning unit. Product analysis was performed with an Agilent Technologies 6890N gas chromatograph (GC) and Thermo Finnigan (Austin, Texas, USA) FOCUS DSQ (dual stage quadrupole) mass spectrometer interfaced with Finnigan FOCUS gas chromatograph (GC-MS).

The reactions were run at least five times, and the data reported here represent the average of these reactions. **1** was generated by literature methods[24c] and **2**, **4**, and **6** were prepared by reacting $[Fe^{II}(L)](CF_3SO_3)_2$ or $[Fe^{II}(TPA)](ClO_4)_2$ (2 mM) with 3 equivalents of peracetic acid in $CH_3CN$ at 0 °C or −40 °C. **3**, **5**, and **7** were prepared by reacting $[Fe^{II}(L)(CF_3SO_3)_2]$ (2 mM) with excess of solid PhIO in $CH_3CN$ at 0 °C. The reactions of $[Fe^{IV}(O)(N4Py)]^{2+}$ (**7**, 1 mM) were followed by monitoring UV/Vis spectral changes of reaction solutions at 695 nm, with a Hewlett Packard 8453 spectrophotometer equipped with a cryostat system. Subsequently, appropriate amounts of substrates were added to the reaction solutions at −40 °C. After the completion of reactions, pseudo-first-order fitting of the kinetic data allowed us to determine $k_{obs}$ values.

For the single-mixing experiments by a Hi-Tech Scientific SF-61 DX2 cryogenic stopped-flow spectrophotometer, a syringe was charged with the intermediates of (**2–6**), and then a second syringe was charged with substrates in $CH_3CN$. The solutions were loaded into the stopped-flow spectrophotometer and triggered by simultaneous injection of 120 μL of each syringe to make the reactant concentrations 1.0 mM and 5–60 mM in the intermediate and substrate, respectively, at −40 °C. All reaction traces were collected at 720 nm, 730 nm, 740 nm, and 770 nm, using a 1 cm optical path length at given temperature and the reaction rates were determined under pseudo-first-order conditions. The reaction condition for **1** with substrate was described elsewhere.[24c] The raw kinetic data were treated with KinetAsyst 3 (Hi-Tech Scientific) and Specfit/32 Global Analysis System software from Spectrum Software Associates.

Product analysis for the oxidation of 1,4-cyclohexadiene (CHD) by the intermediates (**1**-**7**) was performed by GC and GC-MS, and product yields were determined by comparison against standard curves prepared with a known authentic sample. Benzene, which was the desaturated product, was obtained as a sole product (ca. 70–100 %).

## Acknowledgements

M.S.S. thanks the NRF of Korea through Basic Research Program (2010-0002558), S.S. thanks Israel Science Foundation Grant No. ISF 53/09, and W.N. thanks the NRF of Korea through CRI, GRL (2010-00353), and WCU (R31-2008-000-10010-0) and the 2011 KRICT OASIS Project.

[1] H. Eyring, *J. Chem. Phys.* **1935**, *3*, 107–115.
[2] W. Kohn, L. J. Sham, *Phys. Rev.* **1965**, *140*, A1133–A1138.
[3] a) J. N. Harvey, *Faraday Discuss.* **2010**, *145*, 487–505; b) C. L. McMullin, J. Jover, J. N. Harvey, N. Fey, *Dalton Trans.* **2010**, *39*, 10833–10836.
[4] J. M. Mayer, *Acc. Chem. Res.* **2011**, *43*, 36–46.
[5] S. Grimme, J. Antony, S. Ehrlich, H. Krieg, *J. Chem. Phys.* **2010**, *132*, 154104.
[6] a) Y. Morimoto, H. Kotani, J. Park, Y.-M. Lee, W. Nam, S. Fukuzumi, *J. Am. Chem. Soc.* **2011**, *133*, 403–405; b) D. Janardanan, D. Usharani, H. Chen, S. Shaik, *J. Phys. Chem. Lett.* **2011**, *2*, 2610–2617; c) A. J. Johansson, M. R. A. Blomberg, P. E. M. Siegbahn, *J. Phys. Chem. C* **2007**, *111*, 12397–12406; d) H. Chen, W. Z. Lai, S. Shaik, *J. Phys. Chem. Lett.* **2010**, *1*, 1533–1540.
[7] a) D. Schröder, S. Shaik, H. Schwarz, *Acc. Chem. Res.* **2000**, *33*, 139–145; b) D. Janardanan, Y. Wang, P. Schyman, L. Que, Jr., S. Shaik, *Angew. Chem.* **2010**, *122*, 3414–3417; *Angew. Chem. Int. Ed.* **2010**, *49*, 3342–3345; c) S. Shaik, H. Hirao, D. Kumar, *Acc. Chem. Res.* **2007**, *40*, 532–542; d) H. Hirao, K. Morokuma, *J. Am. Chem. Soc.* **2010**, *132*, 17901–17909.
[8] H. Hirao, L. Que, Jr., W. Nam, S. Shaik, *Chem. Eur. J.* **2008**, *14*, 1740–1756.
[9] a) K. M. Smith, R. Poli, J. N. Harvey, *New J. Chem.* **2000**, *24*, 77–80; b) J. N. Harvey, S. Grimme, M. Woeller, S. D. Peyerimhoff, D. Danovich, S. Shaik, *Chem. Phys. Lett.* **2000**, *322*, 358–362; c) Y. Shiota, K. Yoshizawa, *J. Chem. Phys.* **2003**, *118*, 5872–5879; d) D. Danovich, S. Shaik, *J. Am. Chem. Soc.* **1997**, *119*, 1773–1786; e) M. Y. M. Pau, J. D. Lipscomb, E. I. Solomon, *Proc. Natl. Acad. Sci. USA* **2007**, *104*, 18355–18362; f) X.-L. Sun, X.-R. Huang, J.-L. Li, R.-P. Huo, C.-C. Sun, *J. Phys. Chem. A* **2012**, *116*, 1475–1485; g) R. Prabhakar, P. E. M. Siegbahn, B. F. Minaev, H. Ågren, *J. Phys. Chem. B* **2002**, *106*, 3742–3750.
[10] P. E. M. Siegbahn, *J. Biol. Inorg. Chem.* **2006**, *11*, 695–701.
[11] J. Ho, A. Klamt, M. L. Coote, *J. Phys. Chem. A* **2010**, *114*, 13442–13444.
[12] F. Claeyssens, J. N. Harvey, F. R. Manby, R. A. Mata, A. J. Mulholland, K. E. Ranaghan, M. Schütz, S. Thiel, W. Thiel, H.-J. Werner, *Angew. Chem.* **2006**, *118*, 7010–7013; *Angew. Chem. Int. Ed.* **2006**, *45*, 6856–6859.
[13] a) J. Rittle, M. T. Green, *Science* **2010**, *330*, 933–937; b) S. Shaik, D. Kumar, S. P. de Visser, A. Altun, W. Thiel, *Chem. Rev.* **2005**, *105*, 2279–2328.
[14] N. C. Veitch, *Phytochemistry* **2004**, *65*, 249–259.
[15] D. J. Stuehr, O. W. Griffith, in *Adv. Enzymol. Relat. Areas Mol. Biol.*, John Wiley & Sons, Inc. **2006**, pp. 287–346.
[16] P. C. A. Bruijnincx, G. van Koten, R. J. M. Klein Gebbink, *Chem. Soc. Rev.* **2008**, *37*, 2716–2744.
[17] J. M. Bollinger, J. C. Price, L. M. Hoffart, E. W. Barr, C. Krebs, *Eur. J. Inorg. Chem.* **2005**, 4245–4254.
[18] L. M. Hoffart, E. W. Barr, R. B. Guyer, J. M. Bollinger, C. Krebs, *Proc. Natl. Acad. Sci. USA* **2006**, *103*, 14738–14743.
[19] D. P. Galonić, E. W. Barr, C. T. Walsh, J. M. Bollinger, C. Krebs, *Nat. Chem. Biol.* **2007**, *3*, 113–116.
[20] a) W. Nam, *Acc. Chem. Res.* **2007**, *40*, 522–531; b) A. S. Borovik, *Chem. Soc. Rev.* **2011**, *40*, 1870–1874.
[21] H. Hirao, D. Kumar, L. Que, Jr., S. Shaik, *J. Am. Chem. Soc.* **2006**, *128*, 8590–8606.
[22] J. Kaizer, E. J. Klinker, N. Y. Oh, J.-U. Rohde, W. J. Song, A. Stubna, J. Kim, E. Münck, W. Nam, L. Que, Jr., *J. Am. Chem. Soc.* **2004**, *126*, 472–473.

  

[23] a) M. H. V. Huynh, T. J. Meyer, *Chem. Rev.* **2007**, *107*, 5004–5064; b) J. J. Warren, T. A. Tronic, J. M. Mayer, *Chem. Rev.* **2010**, *110*, 6961–7001.

[24] a) M. R. Bukowski, K. D. Koehntop, A. Stubna, E. L. Bominaar, J. A. Halfen, E. Münck, W. Nam, L. Que, Jr., *Science* **2005**, *310*, 1000–1002; b) J.-U. Rohde, J.-H. In, M. H. Lim, W. W. Brennessel, M. R. Bukowski, A. Stubna, E. Münck, W. Nam, L. Que, Jr., *Science* **2003**, *299*, 1037–1039; c) M. S. Seo, N. H. Kim, K.-B. Cho, J. E. So, S. K. Park, M. Clémancey, R. Garcia-Serres, J.-M. Latour, S. Shaik, W. Nam, *Chem. Sci.* **2011**, *2*, 1039–1045; d) M. H. Lim, J.-U. Rohde, A. Stubna, M. R. Bukowski, M. Costas, R. Y. N. Ho, E. Münck, W. Nam, L. Que, Jr., *Proc. Natl. Acad. Sci. U. S. A.* **2003**, *100*, 3665–3670; e) J. Yoon, S. A. Wilson, Y. K. Jang, M. S. Seo, K. Nehru, B. Hedman, K. O. Hodgson, E. Bill, E. I. Solomon, W. Nam, *Angew. Chem.* **2009**, *121*, 1283–1286; *Angew. Chem. Int. Ed.* **2009**, *48*, 1257–1260; f) N. Y. Oh, Y. Suh, M. J. Park, M. S. Seo, J. Kim, W. Nam, *Angew. Chem.* **2005**, *117*, 4307–4311; *Angew. Chem. Int. Ed.* **2005**, *44*, 4235–4239; g) J. Bautz, P. Comba, C. Lopez de Laorden, M. Menzel, G. Rajaraman, *Angew. Chem.* **2007**, *119*, 8213–8216; *Angew. Chem. Int. Ed.* **2007**, *46*, 8067–8070; h) P. Comba, S. Fukuzumi, H. Kotani, S. Wunderlich, *Angew. Chem.* **2010**, *122*, 2679–2682; *Angew. Chem. Int. Ed.* **2010**, *49*, 2622–2625; i) A. Thibon, J.-F. Bartoli, S. Bourcier, F. Banse, *Dalton Trans.* **2009**, 9587–9594; j) D. C. Lacy, R. Gupta, K. L. Stone, J. Greaves, J. W. Ziller, M. P. Hendrich, A. S. Borovik, *J. Am. Chem. Soc.* **2010**, *132*, 12188–12190.

[25] D. Janardanan, D. Usharani, S. Shaik, *Angew. Chem.* **2012**, 124, 4497–4501; *Angew. Chem. Int. Ed.* **2012**, 51, 4421–4425.

[26] a) J. N. Harvey, M. Aschi, H. Schwarz, W. Koch, *Theor. Chem. Acc.* **1998**, *99*, 95–99; b) R. Poli, J. N. Harvey, *Chem. Soc. Rev.* **2003**, *32*, 1–8.

[27] V. W. Manner, A. D. Lindsay, E. A. Mader, J. N. Harvey, J. M. Mayer, *Chem. Sci.* **2012**, *3*, 230–243.

[28] a) A. D. Becke, *Phys. Rev. A* **1988**, *38*, 3098; b) A. D. Becke, *J. Chem. Phys.* **1993**, *98*, 1372–1377; c) A. D. Becke, *J. Chem. Phys.* **1993**, *98*, 5648–5652; d) C. Lee, W. Yang, R. G. Parr, *Phys. Rev. B* **1988**, *37*, 785–789; e) P. J. Hay, W. R. Wadt, *J. Chem. Phys.* **1985**, *82*, 299–310.

[29] a) J. England, M. Martinho, E. R. Farquhar, J. R. Frisch, E. L. Bominaar, E. Münck, L. Que, Jr., *Angew. Chem.* **2009**, *121*, 3676–3680; *Angew. Chem. Int. Ed.* **2009**, *48*, 3622–3626; b) K. Ray, J. England, A. T. Fiedler, M. Martinho, E. Münck, L. Que, Jr., *Angew. Chem.* **2008**, *120*, 8188–8191; *Angew. Chem. Int. Ed.* **2008**, *47*, 8068–8071; c) Y. Wang, K. Han, *J. Biol. Inorg. Chem.* **2010**, *15*, 351–359.

[30] a) R. P. Bell, *Proc. R. Soc. London Ser. A* **1936**, *154*, 414–429; b) M. G. Evans, M. Polanyi, *Trans. Faraday Soc.* **1938**, *34*, 11–24.

[31] S. Shaik, H. Chen, D. Janardanan, *Nat. Chem.* **2011**, *3*, 19–27.

[32] M. J. Frisch, G. W. Trucks, H. B. Schlegel, G. E. Scuseria, M. A. Robb, J. R. Cheeseman, G. Scalmani, V. Barone, B. Mennucci, G. A. Petersson, H. Nakatsuji, M. Caricato, X. Li, H. P. Hratchian, A. F. Izmaylov, J. Bloino, G. Zheng, J. L. Sonnenberg, M. Hada, M. Ehara, K. Toyota, R. Fukuda, J. Hasegawa, M. Ishida, T. Nakajima, Y. Honda, O. Kitao, H. Nakai, T. Vreven, J. A. Montgomery, J. E. Peralta, F. Ogliaro, M. Bearpark, J. J. Heyd, E. Brothers, K. N. Kudin, V. N. Staroverov, R. Kobayashi, J. Normand, K. Raghavachari, A. Rendell, J. C. Burant, S. S. Iyengar, J. Tomasi, M. Cossi, N. Rega, J. M. Millam, M. Klene, J. E. Knox, J. B. Cross, V. Bakken, C. Adamo, J. Jaramillo, R. Gomperts, R. E. Stratmann, O. Yazyev, A. J. Austin, R. Cammi, C. Pomelli, J. W. Ochterski, R. L. Martin, K. Morokuma, V. G. Zakrzewski, G. A. Voth, P. Salvador, J. J. Dannenberg, S. Dapprich, A. D. Daniels, Farkas, J. B. Foresman, J. V. Ortiz, J. Cioslowski, D. J. Fox, *Gaussian 09*, *Revision B.01*, Gaussian Inc., **2009**.

[33] W. L. F. Armarego, C. L. L. Chai, *Purification of Laboratory Chemicals,* 5th ed., Elsevier, **2003**.

[34] O. Bortolini, S. Campestrini, F. Di Furia, G. Modena, *J. Org. Chem.* **1987**, *52*, 5093–5095.

[35] H. Saltzman, J. G. Sharefkin, *Organic Syntheses, Collection, Vol. V*, Wiley & Sons, New York, **1973**.

[36] G. T. Rowe, E. V. Rybak-Akimova, J. P. Caradonna, *Inorg. Chem.* **2007**, *46*, 10594–10606.

Received: January 10, 2012
Revised: April 20, 2012
Published online: June 19, 2012

  